RESEARCH PAPER

Methyl orange degradation using nano-$LaMnO_3$ as a green catalyst under the mild conditions

Neda Rekavandi, Azim Malekzadeh, Elham Ghiasi

School of Chemistry, Damghan University, Damghan, Iran

ARTICLE INFO

Article History:
Received 05 November 2018
Accepted 19 January 2019
Published 15 June 2019

Keywords:
$LaMnO_3$ Nano-Perovskite
Degradation
Azo Pollutants
Sol-Gel Method

ABSTRACT

This study was conducted to investigate the use of cubic $LaMnO_3$ nano-perovskite as a green catalyst for the degradation of an aqueous solution of methyl orange under different conditions. Nanoscale cubic lanthanum manganite with the particle size of ~20 nm was successfully synthesized via citrate sol-gel method. The sample was characterized using the FT-IR and UV-Vis spectroscopy, XRD, SEM, and TEM analyses. The particle size of catalyst was calculated by Scherer equation using data of XRD analysis. The calculations along with an analysis of SEM and TEM confirm the formation of nanosized perovskite phase. The behavior of this nanocatalyst for degradation of an aqueous solution of methyl orange was investigated at wavelengths of 300-700 nm. The effects of the type and different amounts of acid, the absorbent content, pH, and temperature were studied to obtain the optimal conditions of degradation. The prepared sample shows a suitable activity for the methyl orange degradation under dark (~90%) condition. The solar catalytic degradation is faster and goes up to about 100% after 60 min, indicating a different reaction pathway with less activation energy. Pre-visible-light degradation is the basis of catalytic activity of lanthanum manganite. A parallel photocatalytic reaction, however, is an almost simpler way to destroy the azo dyes over $LaMnO_3$ nanoperovskite, which makes the $LaMnO_3$ as a proper photocatalyst for degradation.

How to cite this article
Rekavandi N, Malekzadeh A, Ghiasi E. Methyl orange degradation using nano-$LaMnO_3$ as a green catalyst under the mild conditions. Nanochem Res, 2019; 4(1):1-10. DOI: 10.22036/ncr.2019.01.001

INTRODUCTION

Serious environmental problems are caused due to the discharge of a large quantity of wastewater from industries [1]. Organic substances such as dyes in wastewater are among the sources of environmental pollution. Increasing the availability of procedures to control or eliminate this type of pollution is a challenging issue in this regard. Removal of dyes from industrial wastewaters is done with different physical-chemical methods [2]. Aromatic azo dyes form about half of the global dye production. The molecular structure of these compounds contains a -N=N- bond. About 15% of the aromatic azo dyes enter the wastewaters during dyeing operation processes.

Photocatalytic degradation of dyes on the surface of metal oxides has been intensively studied and is known as a way to solve environmental problems [3-4]. A large band gap restricts the use of metal oxides such as TiO_2 with many known advantages. Utilization of solar radiation energy is limited because a very small amount of UV radiation reaches the earth [5]. Thus, semiconductors with narrower band gap for harvesting the sunlight or ones that act in the ambient conditions are preferred. To develop more efficient catalysts, there is an urgent need for catalytic systems, which are able to operate effectively under visible light irradiation or ambient conditions. In this regard, the use of semiconductor photocatalytic visible light has drawn much attention [6,7].

A catalytic destruction is an environment-

* Corresponding Author Email: *malekzadeh@du.ac.ir*

friendly approach without any pollution. Choosing a cheap catalyst with high-efficiency degradation in normal circumstances is a big problem in this regard. Perovskites-type oxides with the formula of ABO_3 have been extensively investigated as catalysts for many processes [8,9]. Properties such as non-toxicity, ease of use, and high resistance against water, organic, acidic, and alkaline solvents have made perovskites a suitable compound for degradation of pollutants.

Methyl orange with molecular formula $C_{14}H_{14}N_3NaSO_3$ is an example of the azo dyes. Photocatalytic activity of lanthanum manganite, prepared in the presence of citric acid, was evaluated by the photodegradation of aqueous methyl orange [10]. A well-formed perovskite structure was obtained over synthesis of the lanthanum manganite in the presence of citric acid [11]. The superior oxidation catalytic performance of this substance is attributed to its higher specific surface area, better low-temperature reducibility, and concentration of surface adsorbed oxygen species.

In this study, the synthesis of nanosized cubic lanthanum manganite is reported via the sol-gel method using citric acid as a gelling agent. In citrate Sol-Gel method, an organic precursor forms through metallic cations homogeneously distributed throughout the matrix. This synthetic technique can be easily controlled and is more convenient for the synthesis of pure mixed metal oxides nanocrystallites. The spectroscopic and technological characterization and also band gap calculation of sample are also discussed in this work. Further, the activity of the sample for degradation of an aqueous solution of the methyl orange is studied under dark (non-solar) and solar conditions. The catalytic (non-solar) and photocatalytic (solar) activity of $LaMnO_3$ are a challenge. A comparison was made to show if the dark activity of the sample is comparable to that in the solar for degradation of aqueous solution of methyl orange. Factors affecting the catalytic degradation, including the amount of catalyst, initial dye concentration, and pH of the solution, were also investigated.

EXPERIMENT

All the materials used in our experiments were of analytical grade and were used as received without further purification. The $LaMnO_3$ sample was prepared using citrate sol-gel method [12]. Metal nitrates were used as precursors to prepare lanthanum manganite perovskite-type oxide. First, equimolar amounts of metal nitrates were dissolved in 10 mL distilled water in a beaker. Citric acid (CA) was dissolved in 10 mL of distilled water and added to the metal nitrates solution at room temperature. The CA molar ratio was selected to be equal to the total number of moles of nitrate ions. The solution was evaporated at 80°C overnight. The spongy and friable materials obtained were completely powdered and subsequently dried at 160°C overnight. The product was completely powdered and was calcined at 700°C for 5 h.

The FT-IR spectra of the sample were recorded in a PERKIN-ELMER FT-IR spectrometer in the wavenumber range of 450-2000 cm^{-1}. X-ray diffraction (XRD) pattern of the freshly calcined sample was recorded in a Bruker AXS diffractometer D8 ADVANCE with Cu Kα radiation filtered by a nickel monochromator and operated at 35 KV and 35 mA in the range of $2\theta = 10\text{-}80°$. Scanning electron microscopy (SEM) was carried out using a Philips XL30 instrument to investigate the morphology of the samples. The particle size of the sample was calculated by the Scherrer equations using the XRD data and was measured by the transmission electron microscopy (TEM) (CM120, Philips), operating at 120 kV. The particle size of the sample was also measured by a particle size analyzer (Cordouan Technologies Model VASCO). The electronic absorption spectrum was recorded by an Analytik Jena UV–Vis spectrometer.

The degradation experiments were carried out under dark and solar conditions. In an experiment, 20 ml of a fresh aqueous solution of methyl orange, denoted as MO later on, with the initial concentration of 6.5 ppm was placed in a 25 mL round bottom flask. The catalyst was added to the solution and the suspension was stirred. The mixture was centrifuged at random intervals of time. About 3 mL of solution was used for the spectroscopy study. After measurements, the solution was returned to the mixture. The absorption was converted to the concentration using a standard curve. The percentage of degradation of the MO was calculated using the following equation:

$$D\% = \frac{(C_0 - C_t)}{C_0} \times 100$$

where C_0 and C_e are the initial and time "t" concentrations of the solution, respectively. The pH of the mixtures was adjusted using a dilute solution of nitric acid and sodium hydroxide. The hydrogen peroxide and air bubbling were used to study the

effect of the oxidant on degradation. For comparison, a blank run was carried out without catalyst for all degradation studies.

RESULTS AND DISCUSSION

Catalyst characterization

The physical properties of the catalyst sample were determined by SEM, XRD, FT-IR, and electron absorption spectroscopies methods. FT-IR spectra of the crystal sample are shown in Fig. 1a. The band related to 616 cm^{-1} associates with vibrations mode of Mn-O-Mn or Mn-O bond [12-14]. A shoulder at 580 cm^{-1} and a peak at 490 cm^{-1} can be related to a tilted cubic structure, i.e., rhombohedral, and Mn_3O_4 crystals, respectively. Besides, the peak of 1384 cm^{-1} is related to the asymmetric elongation of O-C-O vibration. Hence, it is suggested the presence of a tetragonal carbonate (La_2CO_5 ($La_2O_2CO_3$)) in the sample.

Lanthanum manganite structure consists of a close-packed LaO_3 lattice with Mn in the octahedral sites of oxygen (O_6) [15]. Fig. 2 shows the wide-angle XRD pattern of the as-prepared lanthanum manganite sample and the used one after degradation study. The data were analyzed using a commercial X-pert package and FULLPROF program. The diffraction peaks match with the X-pert high score PDF (code: 01-075-0440), indicating the formation of a cubic $LaMnO_3$ perovskite phase with a space group of Pm-3m and a = 3.8800 Å cell parameter. A FULLPROF analysis distinguishes it with a = 3.8723 Å corrected perovskite. Despite observation of the carbonate and metal oxide in the FT-IR analysis, no diffraction peaks were assigned to such impurities. In this regard, the XRD data was matched with the formation of a single phase perovskite. The absence of carbonate species identified in FT-IR study in XRD spectrum can be related to less amount of non-perovskite species in the sample. Results show that the perovskite structure remains unchanged after degradation. The small displacement of the catalyst peak position used in comparison to the newly created is related to the symmetry change during the degradation. Data of the XRD were used to calculate the crystallite size of the perovskite phase. It was calculated to be ~22 nm using the Scherrer equation (Eq. 1) [14].

$$D = \frac{k \cdot \lambda}{\beta \cdot cos\theta} \quad (1)$$

The SEM and TEM micrographs, particle size distribution histograms obtained according to the TEM result, and result of PSA analysis of the prepared sample are presented in Fig. 3. The surface characterization of sample was performed using SEM micrographs. The sample contains particles with a rather spherical shape. The citric acid prevents agglomeration of the particles to a large extent [11,12], due to releasing of a large amount of gaseous species during the combustion of citric acid used in the preparation process at high temperature. The morphology and particle size of sample were investigated by TEM which shows the same morphology as the SEM image with an average primary particle size around 20 nm. The results are in close agreement with those of Scherrer equation and XRD line profile. The particle size distribution (PSD) of sample (Fig. 3) was obtained using the cumulants method. It is related to a dispersed sample in water. The mean diameter of sample is followed to be ~16

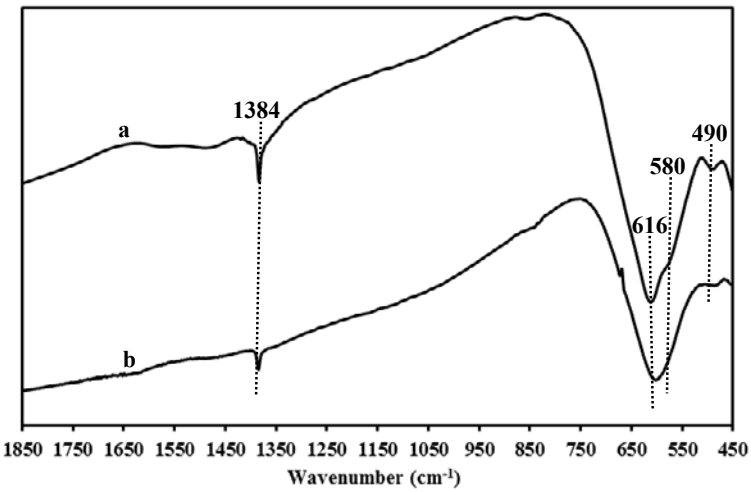

Fig. 1. The infrared spectrum of the prepared crystalline $LaMnO_3$ sample (a) and the used one after degradation (b).

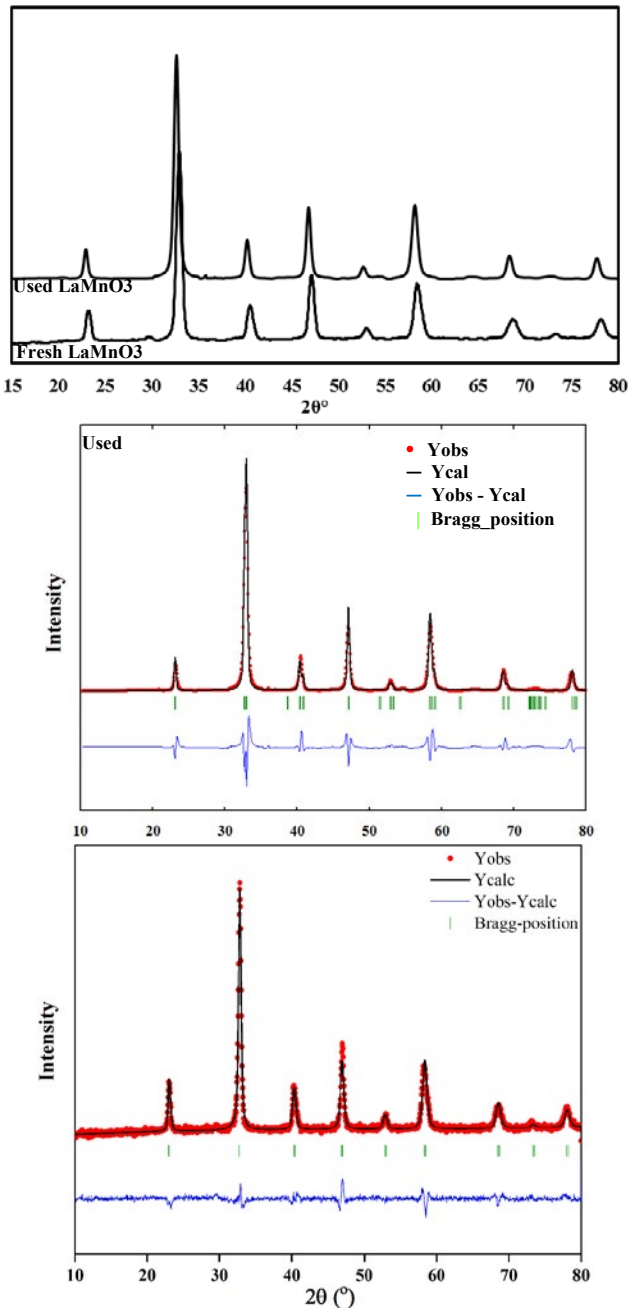

Fig. 2. The XRD patterns of the fresh and used samples and their Rietveld analysis. The circle signs represent the raw data. The solid line represents the calculated profile. Vertical bars indicate the position of Bragg peaks for the cubic $LaMnO_3$ sample. The lowest curve is the difference between the observed and the calculated patterns.

nm. Based on the results, the prepared lanthanum manganite is entirely within the nanoscale domain. The particle size, obtained from particle size analyzer, is similar to the calculated particle size from XRD analysis and TEM study. Result shows that the highest percentage of PSD is around 13 nm.

Fig. 4 shows the UV-Visible absorption spectra and plot of band gap for the prepared sample. The band gap energy was calculated using Tauc's equation (Eq. 2).

$$(\alpha h\nu)^n = B\cdot(h\nu - E_g) \quad (2)$$

where α is absorption coefficient, hν is photon

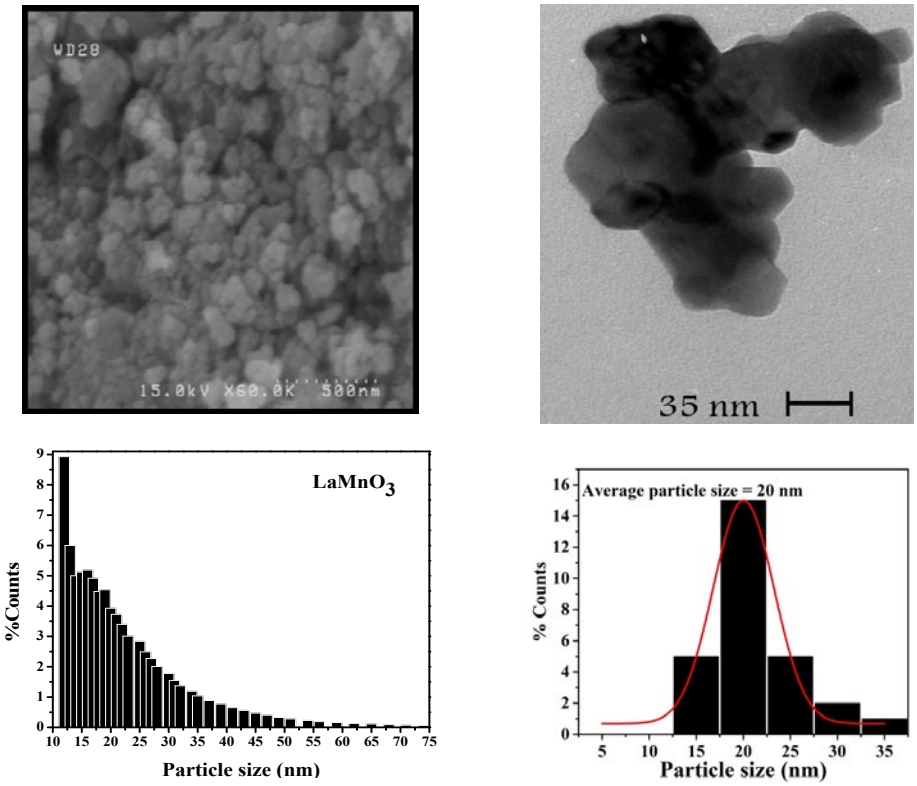

Fig. 3. SEM and TEM micrographs, PSD and size distribution histograms of the prepared crystalline sample.

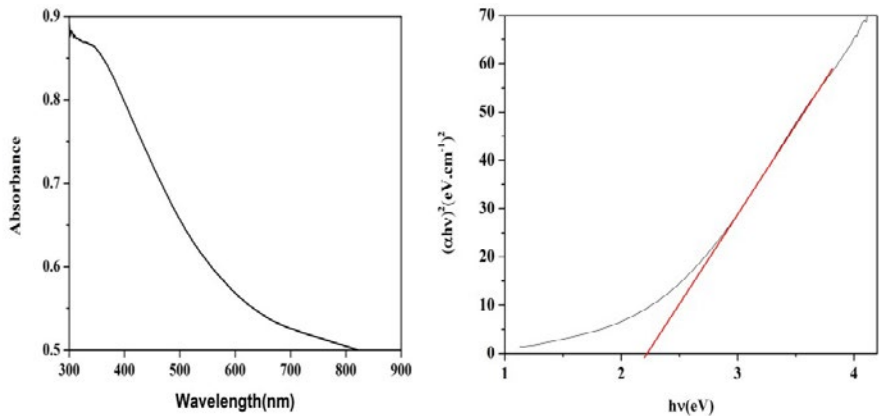

Fig. 4. UV-Vis spectrum and plot of the Tauc's equation for the prepared crystalline nanoparticles.

energy, Eg is band gap energy, B is a constant relative to the material [16]. The exponent "n" denotes the nature of the transition; this exponent is 2 for directly allowed transitions. The band gap of prepared nano-lanthanum manganite sample was calculated to be 2.2 eV (565 nm).

Catalytic and Photocatalytic activity

Dyes are an important class of pollutants. They have a synthetic origin and a complex molecular structure making them more stable. Dyes cause some difficulties when enter into the water; they are not easily biodegraded. The photocatalytic activity of the $LaMnO_3$ sample was evaluated by the photodegradation of aqueous methyl orange exposed to visible light in 38°C [10]. In the present study, the effect of parameters such as acid, pH, adsorbent values, temperature, and oxidant toward

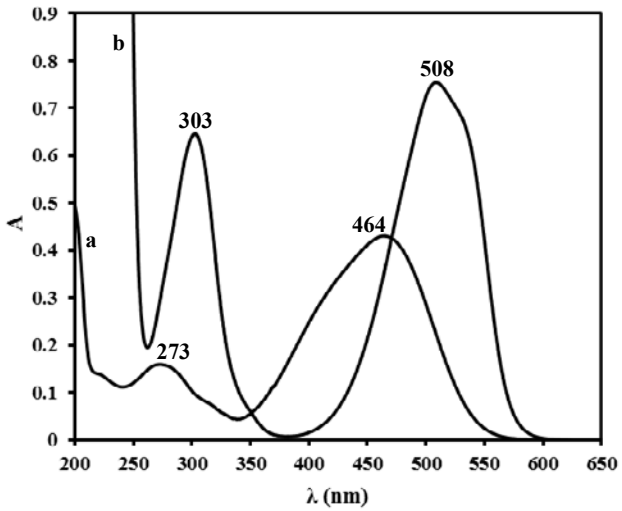

Fig. 5. Electronic absorption spectrum of a 6.5 ppm aqueous solution of MO (a) and an acidic one at pH = 3.1 (b).

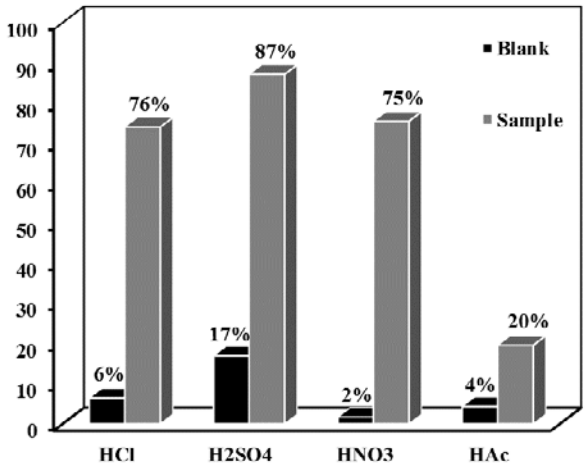

Fig. 6. Degradation of a 6.5 ppm aqueous solution of MO over $LaMnO_3$ catalyst in the presence of different acids. Blank runs (absence of catalyst) are also included.

catalytic, as well as photocatalytic degradation of an aqueous solution of MO over $LaMnO_3$ nano perovskite were studied under darkness and solar conditions. The aim of the present study was to compare the conditions and determine the root of catalytic activity in MO destruction. Azo methyl orange dye is a chemically stable material which is not easily decomposed. [17]. This colored organic complex with a molar mass of 327.33 g/mol is used as an acid-base indicator. Methyl orange is a weak acid with pKa = 3.7. Its color varies from 3.1 to 4.4 in the range of pH. Fig. 5 shows the electron-absorption spectra of 6.5 ppm aqueous solution of fresh and acidic MO in the range of 200-650 nm. As expected from the calculation, the pH of a 6.5 ppm orange colored aqueous solution of MO was measured to be 6.4. The bands at 273 and 464 nm in the electronic absorption spectrum of a fresh aqueous solution of MO are associated with the azo bond (-N=N-) (Fig. 5a). The visible region band of the aqueous solution of MO at 464 nm was used to monitor the reactivity of $LaMnO_3$ nano-perovskite for the degradation of MO under different conditions.

Effect of pH

the pH is an important parameter in controlling the adsorption of species on the solid surface. Here, the effect of the different acids on acidification of the aqueous solution of MO was studied. The results of degradation were compared with a reference. In spite of an almost similar degradation in the

presence of the hydrochloric- sulfuric acids and nitric acid, the results showed that nitric acid has the lowest degradation in the absence of a catalyst (Fig. 6). Accordingly, a 0.1 N nitric acid was used for acidifying the solutions.

The optimum degradation pH was obtained by studying the absorbance band of the visible region of a fresh 6.5 ppm MO solution (464nm) versus pH (Fig. 7). A redshift, accompanied by an increase in the intensity, was observed with a decrease in pH (Figs. 5b and 7). By acidifying a fresh 6.5 ppm of MO solution, the visible absorption band was displaced from 464 nm to 508 nm. The maximum redshift occurred at pH < 3.3 and was about 44 nm at pH = 3.1. The peak intensity of a 6.5 ppm acidic solution of MO (pH = 3.1) was about twice as high as the original solution (pH = 6.4). Thus, the degradation studies were carried out at pH = 3.1.

The prepared adsorbent was characterized for its pH of the point of zero charges (pH_{pzc}). It is another important parameter that can be used in the interpretation of the pH effect on degradation. The "pzc" is a concept associated with the adsorption phenomenon describing the conditions at which the electric charge density on the adsorbent surface is zero and it can be determined using pH Drift Method [18]. Thus, the pH_{pzc} is the pH at which the surface of the catalyst is neutral. According to the results of Fig. 8, the pH_{pzc} of adsorbent was detected to be 3.2. It means that at pH less than 3.2, the surface of $LaMnO_3$ is positively charged and is more susceptible to the electrostatic attraction of

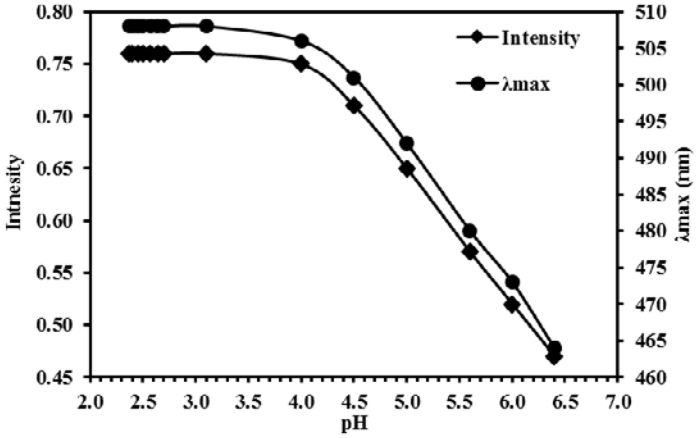

Fig. 7. Changes in position and intensity of the visible region spectrum (λ_{max} = 464 nm) for a 6.5 ppm aqueous solution of methyl orange with pH.

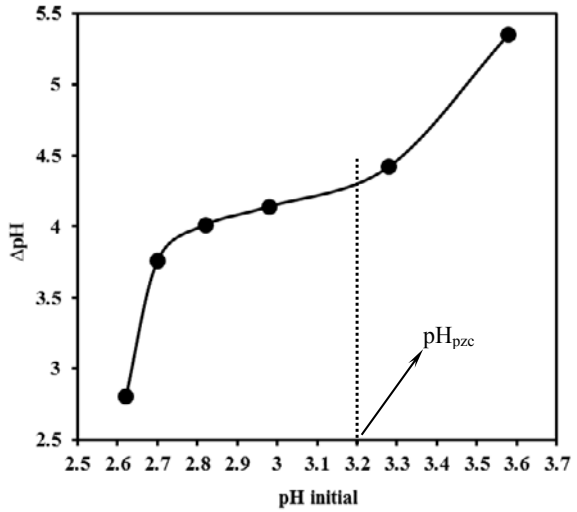

Fig. 8. Determining of the pH_{ZPC} of $LaMnO_3$ catalyst.

anionic species such as methyl orange. The result of pH_{pzc} confirms that the selected pH at 3.1 is suitable for degradation study over the prepared sample.

In Fig. 9, the results of the MO aqueous solution degradation together with prepared nano-catalyst at different pHs are shown. As seen in Fig. 9, in MO aqueous solution, no degradation occurs in 6.7 and 10.5 pHs and the effective pH is acidic ($pH \leq 3.1$). Therefore, this evaluation confirms the results of the test, which indicated the effect of pH on the electron absorption spectra of MO aqueous solution (Fig. 7) and the study of pH_{pzc} (Fig. 8).

The effect of catalyst amount

The degradation of MO aqueous solution on $LaMnO_3$ nono-perovskite with different amounts of nano-catalyst at pH 3.1 was evaluated under darkness and solar conditions (Fig. 10). As seen in Fig. 10, the degradation of azo MO dye is increased by increasing the nano-adsorbent. As a result, degradation shows an ascending trend [19]. It should be noted that by increasing the amount of adsorbent over 10 mg- 10-50 mg nano-catalyst- no significant difference was observed in the degradation rate of MO aqueous solution on $LaMnO_3$ nono-perovskite. Hence, 10 mg was considered as the optimal dose for nano-catalyst. Accordingly, given the constant degradation rate of MO aqueous solution on $LaMnO_3$ nano-particles with more than 10 mg catalyst in darkness, it is not possible to relate the constant degradation rate of MO under the solar condition to light scattering by suspension [20]. This observation is under review. Also, the constant amount of degradation on $LaMnO_3$ nanoparticles with more than 10 mg catalyst in the darkness and solar conditions suggests that the capacity of the $LaMnO_3$ nanoparticles prepared in this study is limited to the MO adsorption. Producing the nanoparticles with a higher surface and higher acceptance capacity is also under consideration.

Temperature effect

The performance of the $LaMnO_3$ nano-perovskite in the degradation of 6.5 ppm methyl orange aqueous solution was investigated at pH = 3.1 and under different darkness and solar conditions at temperatures of 0, 25 and 50°C (Fig. 11). The results show that $LaMnO_3$ nono-perovskite can degrade MO in an acceptable level (60% ~) even in dark conditions and at 0°C. Degradation under sunlight and at around 0°C is about 87%. Similar trends were observed for the MO degradation using $LaMnO_3$ nano-perovskite in different darkness and solar conditions at temperatures of 25°C and 50°C. The destruction of MO under the solar conditions at 25°C and 50°C is more than 96% while in the darkness, it is less than 90%. The results indicate that although the $LaMnO_3$ nano-perovskite has an acceptable performance in the degradation process even in darkness and 0°C, the solar condition is a more appropriate route for degradation. Accordingly, the $LaMnO_3$ nano-perovskite has a dual function, catalytic activity, and better photocatalytic activity. In other words, its activity to degrade azo dye of methyl orange has an active and suitable path to free light.

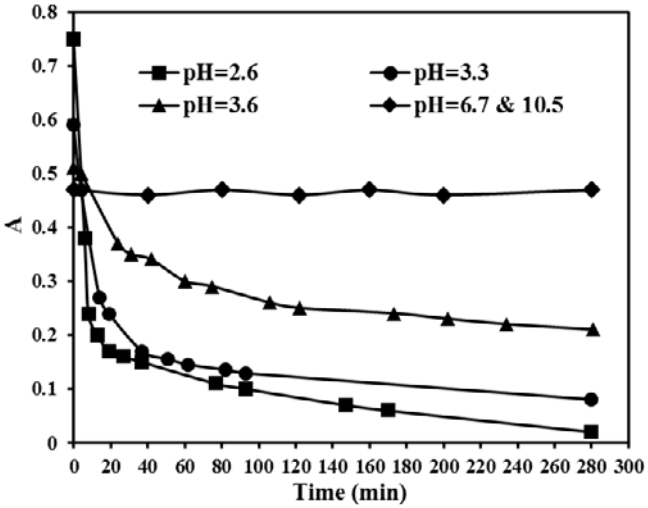

Fig. 9. Degradation studies of a 6.5 ppm aqueous solution of methyl orange over $LaMnO_3$ catalyst at different pHs under darkness condition at 25°C. The pH of the solution was adjusted by addition of dilute solution of HNO_3 or NaOH.

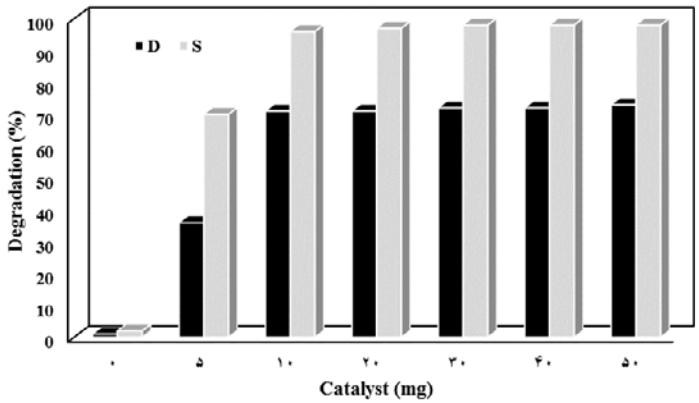

Fig. 10. Effect of the adsorbent amount over degradation of MO (20 mL solution of 6.5 ppm MO, pH = 3.1, t = 60 min).

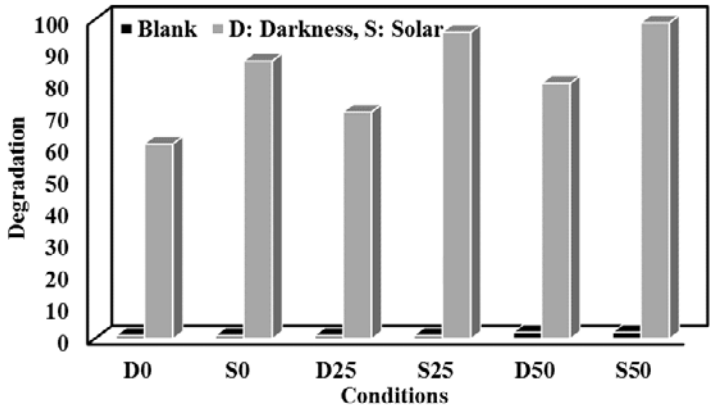

Fig. 11. Results of methyl orange destruction under darkness (D) and solar (S) conditions after 60 min. The studies were carried out using 6.5 ppm aqueous solutions of methyl orange at pH = 3.1 and in the presence of 10 mg catalyst at 0, 25 and 50°C. The numbers that follow "D" and "S" are related to the temperature of degradation. Blank runs, samples without a catalyst, are also included.

The effect of electron receptors

This effect was evaluated by adding H_2O_2 to the or slow air bubbling of the blank solution or the reaction mixture. No changes were observed in the electron absorption spectrum or the degradation rate of MO solution during these experiments. The results show that the presence of an oxidant has no effect on the catalytic or photocatalytic degradation reaction of MO.

Catalyst reuse

Catalytic reuse is of great importance for industrial applications. After each catalytic reaction, the $LaMnO_3$ nanoparticles were separated from the solution, washed with acetone and diethyl ether and then dried at 150°C for 2 hours. The results showed a slight decrease in catalytic activity after each use of $LaMnO_3$ nanoparticles. This reduction in catalytic activity can occur due to the poisoning of active sites, agglomeration of the catalyst particle, or its phase transformation [21]. The catalytic reduction rate after four times use can be ignored.

The results of FT-IR spectroscopic of $LaMnO_3$ nanocatalyst after catalytic and photocatalytic testing are shown in Fig. 1b. The broadband of 616 cm^{-1}, which is attributed to the vibration of the Mn-O octahedral MnO_6 nanoparticle structure, appears more symmetrical [14]. The lack of MO peaks in the FT-IR spectrum of the sample after catalytic and photocatalytic testing indicates the degradation of methyl orange and desorption of degraded species from nano-perovskite, respectively. The results show that nano-lanthanum manganite is an effective catalyst and photocatalyst for degradation of MO. The symmetry of the 616 cm^{-1} peaks of the used sample can be attributed to a more ideal (more symmetrical) cubic structure that was shown to be a distorted cubic structure

(somewhat rhombohedral) for the fresh sample. It seems that by progressing the reaction, the prepared $LaMnO_3$ nano-catalyst is becoming more symmetrical. The results are in line with XRD analysis. This structural change and its impact on the catalytic activity are under review.

CONCLUSION

Distorted cubic nano perovskite of lanthanum manganite ($LaMnO_3$) with a space group of Pm-3m and cell parameter a = 3.88 Å can be prepared via the calcination of a xerogel at 600°C. A corrected cell parameter of a = 3.87 Å was obtained using the FULLPROF analysis. Xerogel was obtained by the citrate sol-gel method using metal nitrate and sequential drying at 80°C and 150°C. The synthesized nano lanthanum manganite shows an acceptable activity for azo methyl orange degradation under no-light conditions. Although a free-light degradation is the starting point of catalytic activity of lanthanum manganite, the degradation of the solar condition is comparable to the destruction of darkness.

CONFLICT OF INTEREST

The authors declare that there is no conflict of interests regarding the publication of this manuscript.

REFERENCES

[1] Coates JF. The sixteen sources of environmental problems in the 21st century. Technological Forecasting and Social Change. 1991;40(1):87-91.

[2] Pirkarami A, Olya ME. Removal of dye from industrial wastewater with an emphasis on improving economic efficiency and degradation mechanism. Journal of Saudi Chemical Society. 2017;21:S179-S86.

[3] Hoffmann MR, Martin ST, Choi W, Bahnemann DW. Environmental Applications of Semiconductor Photocatalysis. Chemical Reviews. 1995;95(1):69-96.

[4] Reza KM, Kurny ASW, Gulshan F. Parameters affecting the photocatalytic degradation of dyes using TiO2: a review. Applied Water Science. 2015;7(4):1569-78.

[5] Fox MA, Dulay MT. Heterogeneous photocatalysis. Chemical Reviews. 1993;93(1):341-57.

[6] Serpone N, Emeline AV. Semiconductor Photocatalysis — Past, Present, and Future Outlook. The Journal of Physical Chemistry Letters. 2012;3(5):673-7.

[7] Hernández-Ramírez A, Medina-Ramírez I. Photocatalytic semiconductors: Springer; 2016.

[8] Royer S, Duprez D, Can F, Courtois X, Batiot-Dupeyrat C, Laassiri S, et al. ChemInform Abstract: Perovskites as Substitutes of Noble Metals for Heterogeneous Catalysis: Dream or Reality. ChemInform. 2014;45(50):no-no.

[9] Labhasetwar N, Saravanan G, Kumar Megarajan S, Manwar N, Khobragade R, Doggali P, et al. Perovskite-type catalytic materials for environmental applications. Science and Technology of Advanced Materials. 2015;16(3):036002.

[10] Shaterian M, Enhessari M, Rabbani D, Asghari M, Salavati-Niasari M. Synthesis, characterization and photocatalytic activity of LaMnO3 nanoparticles. Applied Surface Science. 2014;318:213-7.

[11] Zhang C, Guo Y, Guo Y, Lu G, Boreave A, Retailleau L, et al. LaMnO3 perovskite oxides prepared by different methods for catalytic oxidation of toluene. Applied Catalysis B: Environmental. 2014;148-149:490-8.

[12. Ghiasi E, Malekzadeh A, Ghiasi M. Moderate concentration of citric acid for the formation of LaMnO3 and LaCoO3 nano-perovskites. Journal of Rare Earths. 2013;31(10):997-1002.

[13] Kleist W, Maciejewski M, Baiker A. MOF-5 based mixed-linker metal–organic frameworks: Synthesis, thermal stability and catalytic application. Thermochimica Acta. 2010;499(1-2):71-8.

[14] Khazaei M, Malekzadeh A, Amini F, Mortazavi Y, Khodadadi A. Effect of citric acid concentration as emulsifier on perovskite phase formation of nano-sized SrMnO3 and SrCoO3 samples. Crystal Research and Technology. 2010;45(10):1064-8.

[15] Jiang LQ, Guo JK, Liu HB, Zhu M, Zhou X, Wu P, et al. Prediction of lattice constant in cubic perovskites. Journal of Physics and Chemistry of Solids. 2006;67(7):1531-6.

[16] Tumuluri A, Naidu KL, Raju KJ. Band gap determination using Tauc's plot for LiNbO3 thin films. Int J Chem Tech Res. 2014; 6(6): 3353-6.

[17] Ghiasi M, Malekzadeh A. Solar photocatalytic degradation of methyl orange over La0.7Sr0.3MnO3 nano-perovskite. Separation and Purification Technology. 2014;134:12-9.

[18] Yang Y, Chun Y, Sheng G, Huang M. pH-Dependence of Pesticide Adsorption by Wheat-Residue-Derived Black Carbon. Langmuir. 2004;20(16):6736-41.

[19] Subash B, Krishnakumar B, Swaminathan M, Shanthi M. Enhanced photocatalytic performance of WO3 loaded Ag–ZnO for Acid Black 1 degradation by UV-A light. Journal of Molecular Catalysis A: Chemical. 2013;366:54-63.

[20] Sotelo JL, Ovejero G, Martínez F, Melero JA, Milieni A. Catalytic wet peroxide oxidation of phenolic solutions over a LaTi1−xCuxO3 perovskite catalyst. Applied Catalysis B: Environmental. 2004;47(4):281-94.